Evaluation of Diffusion Filters for 3D CTA Liver Vessel Enhancement

Ha Manh Luu, Adriaan Moelker, Camiel Klink, Adrienne Mendrik, Wiro Niessen, and Theo van Walsum

Biomedical Imaging Group Rotterdam, Departments of Medical Informatics and Radiology, Erasmus MC, University Medical Center Rotterdam, Dr. Molewaterplein 50, 3015 GE Rotterdam, The Netherlands
haluumanh@erasmusmc.nl

Abstract. We present an evaluation of five diffusion filters for liver vessel enhancement in 3D CTA datasets of the liver. 3D CTA liver images are generally noisy, with limited contrast between vessels and parenchyma, especially for the small vessels. We investigate the performance of five (an)isotropic diffusions filters: Regular Perona-Malik, Coherence-Enhancing Diffusion, Edge-Enhancing Diffusion, Hybrid Diffusion with Continuous Switch and Vessel Enhancing Diffusion on a set of 14 abdominal CTA clinical datasets. The evaluation is based on signal to noise improvement. A parameter optimization is performed on 7 training images, after which the optimal versions of the filters are compared on 7 test images. The results demonstrate that all the diffusion filters improve SNR of the images and Hybrid Diffusion with Continuous Switch and Vessel Enhancing Diffusion gives the largest increase in SNR.

Keywords: Diffusion, HDCS, VED, CED, RPM, EED, 3D CTA, liver vessel.

1 Introduction

Liver vessel analysis is relevant for several clinical applications, a.o. for planning and guidance in minimally invasive interventions. Particularly, segmentation of the portal and hepatic veins is relevant for procedures such as liver surgery, TIPS and RFA. Arterial segmentation is relevant for e.g. chemo-embolization procedures in the liver.

Liver vessel segmentation is challenging because 3D abdominal CTA is noisy, has variable contrast between the vessel and liver parenchyma, and because of the complex topology and varying sizes of the vessels. The quality of the CTA images depends on radiation dose, amount of contrast agent, and timing of data acquisition with respect to dose injection. Image quality could be improved at the expense of increased radiation dose or increased contrast usage, but both strategies are clinically not acceptable.

Several liver vessel segmentation methods have been developed so far, a review of liver vessel segmentation can be found at [1]. Most of the works relating to liver vessel segmentation on 3D clinical CTA use filters to reduce the noise and enhance the vessel structure. Mainly, multi-scale Hessian based filters (Frangi, Sato, Erdt)

H. Yoshida, D. Hawkes, M.W. Vannier (Eds.): Abdominal Imaging 2012, LNCS 7601, pp. 168–177, 2012.

[2, 4, 5, 7] have been used in these studies. However, these studies lack an evaluation on to what extent preprocessing improves the segmentation results. A comparison of multi-scale Hessian based filters can be found at [3], but that study only demonstrates the effect of these Hessian-based filters without any quantitative measure. The study also shows that Hessian-based approaches may not work well at bifurcations and vessels with high curvature.

The purpose of our study is to quantitatively evaluate the effect of diffusion filters on vessel enhancement in 3D CTAs of the liver. We investigate both the optimal filter settings for these filters, and compare the optimal versions of each filter. For the filters, we choose five well-known (an)isotropic diffusion filters: Regular Perona-Malik (RPM), Contrast-Enhancing Diffusion (CED), Edge-Enhancing Diffusion (EED), Vessel-Enhancing Diffusion (VED) and Hybrid Diffusion with Continuous Switch (HDCS). RPM and EED have been applied to 3D rotational angiography images by Meijering et al [10]. They showed that EED works well in smoothing the vessel, while RPM can preserve small vessels. CED, introduced by Weickert [9], can filter tube-like structures. VED was published by Manniesing et al in 2006 [8]. This filter uses Hessian-based multi-scale filter's responses to adjust diffusion scheme. Finally, HDCS was published by Mendrik et al in 2009 [10]. This filter combines both advantages of EED and CED to filter both homogeneous areas and vessel structures.

2 Methodologies

All filters we evaluated are diffusion filters. The main idea of diffusion filters comes from PDE [8] $u_t = \mathrm{div}(D.\nabla u)$ where ∇u is the gradient of the image and D is the diffusion tensor, which steers the diffusion. If the diffusion tensor D is replaced by a scalar-valued diffusivity g the diffusion will be isotropic. Whereas RPM is an isotropic filter, that only changes the amount of smoothing based on local gradient magnitude, the other filters are anisotropic filters, that not only locally change the level, but also the direction of smoothing by adapting the diffusion tensor. Each of the five filters is described in more detail below.

RPM: Perona and Malik (1990) introduced an isotropic nonlinear diffusion as described by $u_t = \mathrm{div}(g(|\nabla u|).\nabla u)$. The scalar-valued diffusivity $g(|\nabla u|)$ is function of the gradient $|\nabla u|$, causing filtering in homogenous areas while retaining edges with high gradient. Catte [10] proposed the following scalar-valued diffusivity function for the non-linear diffusion using Gaussian derivative at scale σ:

$$g(|\nabla u_\sigma|) = 1 - e^{\frac{-C}{(|\nabla u_\sigma|^2/\lambda^2)^4}}, \quad (1)$$

where C = 3.1488 and λ is contrast parameter. The contrast parameter λ acts as threshold scale for gradient $|\nabla u_\sigma|$. If the gradient is large compared to the contrast parameter, i.e $|\nabla u_\sigma|^2 \gg \lambda^2$, this results in $g(|\nabla u_\sigma|) \approx 0$, reducing the amount of diffusion. Therefore strong edges, where the gradient of u is large, are preserved. Parameter σ is the scale of Gaussian gradient. Value of σ should be chosen based on noise variance and the size of the small structures we want to retain.

EED: Weickert et al (1997) included information of orientation in diffusion scheme. Instead of using a scalar diffusivity function, they used a diffusion tensor D which was constructed from the tensor product:

$$J_\rho(\nabla u_\sigma) = K_\rho * (\nabla u_\sigma \nabla u_\sigma{}^{\mathrm{T}}). \quad (2)$$

J_ρ is a positive symmetric matrix. By eigendecomposing $J_\rho = V.M.V^{\mathrm{T}}$, they can extract eigenvalues μ_i (i = 1-3, $\mu_1 > \mu_2 > \mu_3$), the diagonal elements of matrix M, and corresponding direction eigenvectors V_1 , V_2 and V_3. Because eigenvalue μ_1 is the largest eigenvalue, eigenvectors V_1 is in the direction of highest contrast (edges). The diffusion tensor is defined as $D = V.\Lambda.V^{\mathrm{T}}$ with eigenvectors V as the same eigenvectors of tensor product J_ρ. Eigenvalues of diffusion tensor of EED, Λ, are defined as: $\lambda_{e_2} = \lambda_{e_3} = 1$ and

$$\lambda_{e_1} = \begin{cases} 1 & |\nabla u_\sigma| = 0 \\ 1 - e^{\frac{-c}{(|\nabla u|^2/\lambda_e^2)^4}}, & |\nabla u_\sigma| > 0 \end{cases}, \quad (3)$$

where, similar to RPM, C = 3.1488, and λ_e is the contrast parameters. This diffusion tensor results in large isotropic diffusion in flat areas where the gradient is small, and performs almost no diffusion in the direction along which gradient is the highest (V_1). K_ρ in equation (2) acts as smoothing of gradient (Gaussian convolution with kernel ρ). If gradient ∇u_σ has large range of values, ρ should be high enough to smooth the product. Otherwise, ρ should be small enough to capture small changes in gradient.

CED: Weickert (1999) included a coherence factor in diffusion process. The coherent factor is defined as:

$$\kappa = (\mu_1 - \mu_2)^2 + (\mu_2 - \mu_3)^2 + (\mu_3 - \mu_1)^2, \quad (4)$$

This factor measures the relation of each pair of the eigenvalues. If a structure is tubular, V_1 , V_2 direction are in the direction of high contrast and V_3 in the direction of little contrast. Thus in the case of tubular structures, $\mu_1 \approx \mu_2 \gg \mu_3$, and thus κ has high a value. Otherwise, κ has small value. Eigenvalues of diffusion tensor of CED are defined as: $\lambda_{c_1} = \lambda_{c_2} = \alpha$ and

$$\lambda_{c_3} = \begin{cases} \alpha & \kappa = 0 \\ \alpha + (1-\alpha)\exp(-C/\kappa), & \kappa > 0 \end{cases}, \quad (5)$$

where C = 3.1488 and α is very small. For tube-like structures, κ is large, the diffusion mainly occurs in the direction V_3(least contrast). Therefore CED only blurs along tubular structures. For plate-like structures, κ is small, resulting in small isotropic diffusion (depends on α).

HDCS: Mendrik (2009) introduced HDCS as a combination of CED and EED. The main idea is that to use a voting criterion to decide whether local structure is tubular or non–tubular. The structure classifier is defined as:

$$\xi = \mu_1/(\alpha + \mu_2) - \mu_2/(\alpha + \mu_3), \quad (6)$$

where $\alpha = 0.001$ and $(\mu_1 > \mu_2 > \mu_3)$ are eigenvalues of tensor product in equation (2). $\xi \ll 0$ when the structure is tubular, $\xi \approx 0$ when structure is sphere -like (background and noise), and $\xi \gg 0$ when structure is plate-like. The eigenvalues of HDCS diffusion tensor is combination of eigenvalues of EED and CED:

$$\lambda_{\hbar_i} = (1 - \varepsilon)\lambda_{c_i} + \varepsilon\lambda_{e_i}, \tag{7}$$

$$\varepsilon = \exp\left(\frac{\mu_2(\lambda_{\hbar}^2(\xi - |\xi|) - 2\mu_3)}{2\lambda_{\hbar}^4}\right), \tag{8}$$

where $\lambda_{\hbar}$ is contrast parameter. When the local structure is tubular, $\varepsilon \to 0$ and the diffusion is CED-like, for other structures $\varepsilon \to 1$, and diffusion is EED-like.

VED: Manniesing (2006) used the multi-scale Hessian filter response to drive the diffusion. The main idea of the multi-scale Hessian filter is that by using eigenvalues of Hessian matrix, which determine local curvatures, we can distinguish tubular structures from other structures in a multi-scale framework. The output response is a combination of the maximum responses at each scale. Let $V \in [0,1]$ is the output of a multi-scale scale vesselness filter. V should be around 1 inside tubular structures and 0 elsewhere. Assume that $|\lambda_1| < |\lambda_2| < |\lambda_3|$ are eigenvalues of Hessian matrix H, corresponding to eigenvectors Q_1, Q_2 and Q_3, i.e., $H = Q.\Lambda.Q^{\mathrm{T}}$. Then, Q_1 should be the direction of the least curvature (along vessel in case of vessel structure). The diffusion tensor D is defined as $= Q.\Lambda'.Q^{\mathrm{T}}$. Diagonal elements of matrix Λ' can be defined as:

$$\begin{aligned} \lambda'_1 &= 1 + (\omega - 1)V^{1/s}, \\ \lambda'_2 &= \lambda'_3 = 1 + (\varepsilon - 1)V^{1/s}, \end{aligned} \tag{9}$$

where s is a sensitivity parameter which controls the impact of V on λ'_1 ; ω is a parameter larger than 1, which ensures that Q_1 is always the direction of largest diffusion; ε is relative small to allow high isotropic diffusion when $V \approx 0$ (non-vessel structure).

3 Experiments and Evaluations

3.1 Data

We randomly chose 7 training datasets and 7 testing datasets from portal venous phase liver CTAs that were acquired in Erasmus Medical Center, Rotterdam. The datasets have an in-plane pixel size of 0.74 mm x 0.74 mm, 1-1.5 mm slice spacing, 1-2 mm slice thickness, 72-180 axial slices, 512 x 512 pixels per slice. Scanning was performed 60 seconds after the injection of 100 cc intravenous contrast agent with radiation dose of 140 - 320 mAs and control voltage of 80 - 120 kV. The datasets contain portal veins, hepatic veins, tumors, cysts, metastases in different shape and size. Some datasets also contain metal artifacts.

To reduce filtering times, we cropped the datasets into smaller datasets which containing all liver vessels, which resulted in a reduction of around 75 %.

3.2 Evaluation Criteria

We use SNR as a quantitative metric to determine whether the images have improved. We calculate the SNR over a large set of point pairs that were annotated in the vessel and in the background. We follow the following protocol to calculate the SNR:

1. We choose 12 to15 random axial slices within liver region to ensure that number of vessels in those is sufficient (more than 300 vessels per data)
2. In every slice, a trained observer annotated all vessels, which have diameter from 0.74mm (one pixel) to around 10 mm, by clicking one point in the vessel, we call them object points.
3. For each object point, a corresponding nearby points in the liver parenchyma is manually selected, which is at least 5 pixels away from the vessels. We call these background points.
4. The SNR of each pair is calculated as:

$$SNR = 20log10\frac{obj-mean(bgr)}{std(bgr)} \text{ (dB)}, \tag{10}$$

where the standard deviation of the background points is determined in an axial 5x5 ROI around the point.

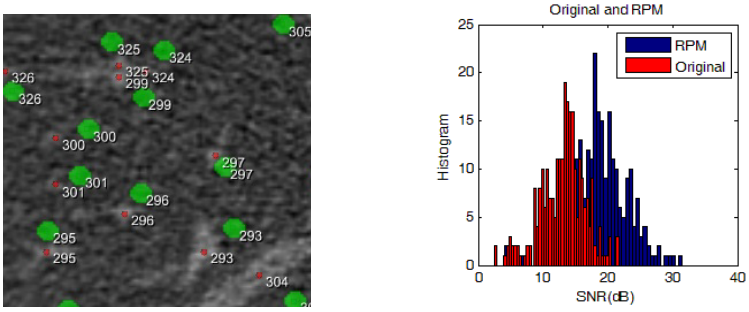

(a) (b)

Fig. 1. (a) The vessel markers for SNR calculation: Small red dots are vessel markers, respectly indexed to big green circles on nearby background arias. (b) SNR histograms of an original image (red) and a diffusion image (gray).

From the SNR of all these pairs in one datasets, we determine the mean and standard deviation, which we use to quantitatively evaluate the filter's results and analyze the effect of the filters on large and small vessels.

3.3 Parameter Optimization

The optimal filter parameters are determined in a training stage. For each of the training datasets, we apply the five filters and tune parameters to get the optimal result, based on the mean SNR over all datasets. For the range of values for each parameter we follow the suggestions of Mendrik et al. [10].

The parameter optimization is performed on Linux cluster which contain 80 2.4GHz-64 bits-cores. For RPM, CED, EED, it takes 10 to 20 seconds per iteration,

while for CED and VED, it takes 30 to 60 seconds per iteration. The maximum number of iteration of all filters is set to 50. All parameter values are described in detail in appendix A.

4 Results

4.1 Optimal Parameters

Fig. 2(a) shows the optimal contrast parameter of EED and Fig. 2(b) presents the curve of SNR versus number of iterations for RPM. Fig 2(a) shows the optimization results for the contrast parameter for EED, which demonstrates that the value of that parameter is dataset – independent, whereas the number of iterations [Fig 2(b)] is dataset-dependent: the more noisy data is, the more number of iteration is required.

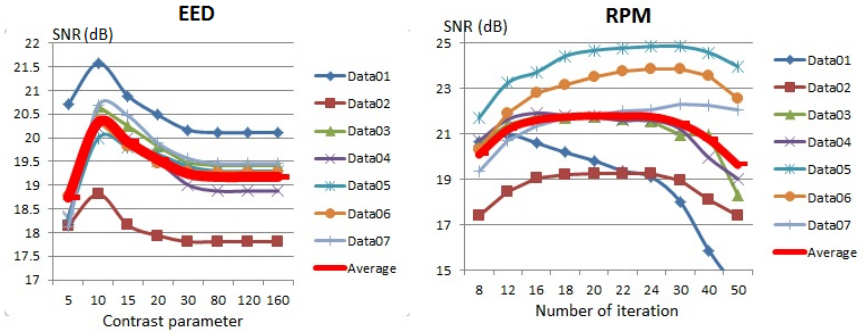

(a) (b)

Fig. 2. (a) The average optimal contrast parameter for EED is at 10 (the highest SNR value of the red curve). (b) The average optimal number of iterations for RPM is around 22.

The optimal parameters resulting from the training step are listed in Table 1.

Table 1. The optimal parameters of the diffusion filters

Filter	Abbr	Optimal Parameters
Regular Perona- Malik	RPM	$\tau = 0.0625$; $\eta = 22$; $\lambda = 10$; $\sigma = 1$
Edge-Enhancing Diffusion	EED	$\tau = 0.0625$; $\eta = 40$; $\lambda_e = 10$; $\sigma = 1$
Coherence-Enhancing Diffusion	CED	$\tau = 0.0625$; $\eta = 50$; $\lambda_c = 5$; $\alpha = 0.001$; $\sigma = 1$; $\rho = 1$
Hybrid Diffusion filter with Continuous Switch	HDCS	$\tau = 0.0625$; $\eta = 40$; $\lambda_c = 5$; $\lambda_e = 10$; $\lambda_h = 10$; $\alpha = 0.001$; $\sigma = 1$; $\rho = 1$
Vessel Enhancing Diffusion	VED	$\tau = 0.0625$; $\eta = 32$; $\omega = 25.0$; $s = 1$; $\varepsilon = 0.01$; $\sigma_{min} = 1$; $\sigma_{max} = 3$; $\nu = 5$; $\alpha = 0.5$; $\beta = 0.5$; $\gamma = 120$

4.2 Filter Comparison

We applied the filters on the 7 test datasets with the optimal parameters from Table 1. Ranking of each diffusion filter are based on average SNR over the test datasets. The

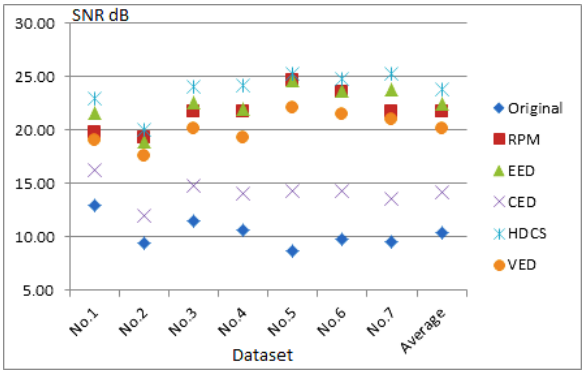

Fig. 3. Ranking on test dataset

results of the overall performance are summarized in Fig. 3. According to the results, HDCS performed better than the other filters.

From Fig. 3, we can see that all filtered results have better SNR than original ones. This also can be seen as SNR histogram in Fig. 1. Fig. 1(b) is an example of SNR histograms of an original image (red) and a diffusion image (gray). The diffusion image's histogram is to the right of the original's one, that means the filter has improved SNR in general.

To visualize the effect of diffusion filters in terms of SNR, we calculated the changes in SNR between every pair of points of the filtered images and those of the original ones. The delta SNR is divided into 3 parts: the red part is smaller than zero, that means at those locations, the diffusion results in a worse SNR.; the yellow part is from zero to mean of SNR, which means that at those locations, the diffusion filter is able to improve SNR; the green points are those where the SNR is larger than the mean of the SNR, which means that there is a large improvement. The results for one dataset are shown in Fig. 4.

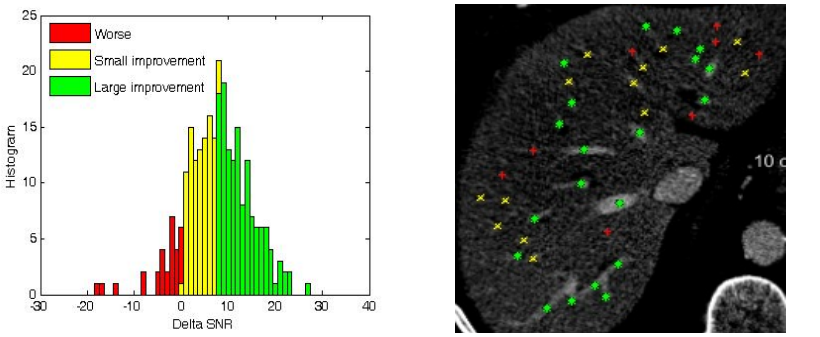

(a) (b)

Fig. 4. (a) Histogram of Delta SNR and (b) vessel marker render, respectly. The yellow part is remarked by yellow x characters; The green part is noted by green asterisks; The red part is represented by red + characters.

5 Discussion

We have optimized and applied five diffusion filters for increasing the SNR in liver vessel CTA images. In the parameter optimization stage, we choose a time step which is quite small, $\tau = 0.0625$, to ensure stability of diffusion scheme. In the experiments, we can see that, when increasing the number of iteration, SNR increases as noise is suppressed. However, when the number of iterations becomes too large, both vessel structure and noise are blurred, which results in an SNR decrease. Around the optimal number of iteration, the SNR curve is quite flat [Fig. 2(b)].

To visually compare the results, outputs of each filter and the unfiltered image are shown in Fig. 5 with the same window-level, we can see that the original image has good contrast but much noise. All of the filters, to some extent, blurred low-contrast smaller-than-1 mm vessels. The reason may be that, in optimization step, at Gaussian scale $\sigma = 1$, large vessels have more SNR improvement than the SNR reduction in the small vessels [Fig. 4 (b)]. Diffusion filters blur noise, improve high contrast vessels but also blur low-contrast small vessel.

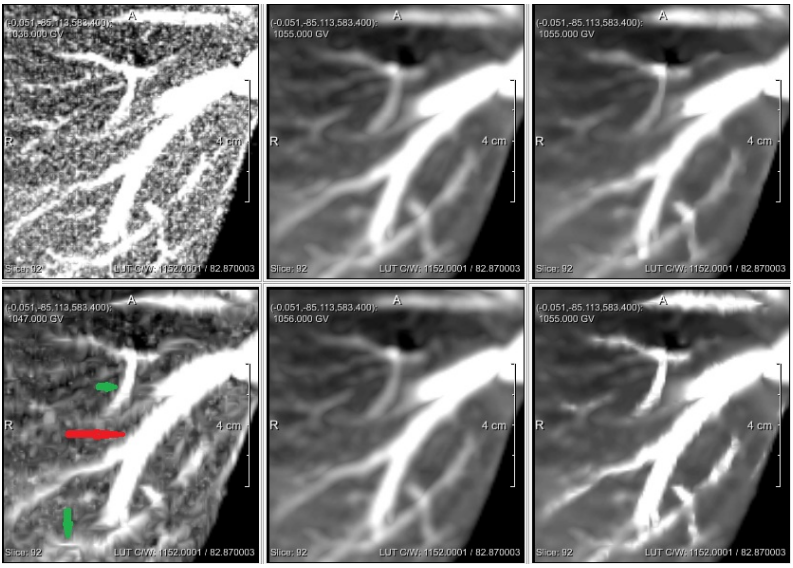

Fig. 5. Maximum intensity projection (7 slices) of the diffusion outputs. Order of top row from left to right: Original, RPM, EED. Order of bottom row from left to right: CED, VED, HDCS.

Also in Fig. 5, EED, VED, and RPM reduce contrast between vessels and background. This effect results from blurring in all directions if gradient or curvature is not high enough to prevent blurring. CED and HDCS not only keep better contrast between vessel and background, but also retain better the structure of small vessels (short-blue green). However, in this study, CED leads to irregular borders of large vessels (long-red arrow). The main reason is that noise at the edges makes the CED tensor consider this noise as small vessels. For HDCS, this effect is not as much as CED because at boundary, EED has some impacts. This effect doesn't influence SNR in general because we only take evaluate the intensity at the center of vessel. In this

study, we used coherent factor $\kappa = (\mu_1 - \mu_2)^2 + (\mu_2 - \mu_3)^2 + (\mu_3 - \mu_1)^2$ for CED as suggested in the original paper by Weickert [1999]. This results in rough effect at boundary of big vessel. In the HDCS paper [10], Mendrik introduced a new coherent factor $\kappa = \left(\mu_2/(\alpha + \mu_3)\right)^4$. This causes the boundaries of large vessels to be smoother compared to the CED version in this study. In further study, we could use that factor to have better adapted for 3D images.

In test stage, CED shows the worse ranking [Fig 3]. The main reason of this ranking is that CED mainly blurs inside the vessel while noise in flat areas is not suppressed much. In contrast, HDCS not only performs well in side vessel as CED does, but also uses the diffusion property of EED, blurring when gradient is small, in flat areas. This quantitative result is in agreement with the conclusion of the qualitative evaluation by Mendrik et al.

This study just shows optimal parameters for global SNR. However at optimal SNR, all the diffusions expose problem with very small and low contrast vessels. Depending on specific clinical application, for instant in RFA (when detection of small vessels is relevant), we can use this study to recognize very small and low contrast vessels, and then optimize setting again.

6 Conclusion

We presented a quantitative evaluation of five diffusion filters, RPM, EED, CED, HDCS and VED on 3D CTA images of the liver. We optimized the relevant parameters of each filter on a training set of seven CTAs. Based on an evaluation on an independent set of seven datasets and using SNR as criterion, we conclude that HDCS filter performs the best over the other filters.

References

1. Lesage, D., Angelini, E.D., Bloch, I., Funka-Lea, G.: A Review of 3D Vessel Lumen Segmentation Techniques: Models, Features and Extraction Schemes. Med. Image Anal. 13, 819–845 (2009)
2. Freiman, M., Joskowicz, L., Sosna, J.: A Variational Method for Vessels Segmentation: Algorithm and Application to Liver Vessels Visualization. In: Proc. of SPIE, vol. 7261, p. 72610H (2009)
3. Drechsler, K., Laura, C.O.: Comparison of Vesselness Functions for Multiscale Analysis of the Liver Vasculature. In: 10th IEEE International Conference on Information Technology and Applications in Biomedicine, pp. 1–5. IEEE Press, New York (2010)
4. Erdt, M., Raspe, M., Suehling, M.: Automatic Hepatic Vessel Segmentation Using Graphics Hardware. In: Dohi, T., Sakuma, I., Liao, H. (eds.) MIAR 2008. LNCS, vol. 5128, pp. 403–412. Springer, Heidelberg (2008)
5. Lehmann, K.S., Ritz, J.P., Valdeig, S., Schenk, A., Holmer, C., Peitgen, H.O., Buhr, H.J., Frericks, B.B.: Portal Vein Segmentation of a 3D-Planning System for Liver Surgery - In Vivo Evaluation in a Porcine Model. Ann. Surg. Oncol. 15, 1899–1907 (2008)
6. Selle, D., Preim, B., Schenk, A., Peitgen, H.O.: Analysis of Vasculature for Liver Surgical Planning. IEEE Trans. Med. Imaging 21, 1344–1357 (2002)

7. Alhonnoro, T., Pollari, M., Lilja, M., Flanagan, R., Kainz, B., Muehl, J., Mayrhauser, U., Portugaller, H., Stiegler, P., Tscheliessnigg, K.: Vessel Segmentation for Ablation Treatment Planning and Simulation. In: Jiang, T., Navab, N., Pluim, J.P.W., Viergever, M.A. (eds.) MICCAI 2010, Part I. LNCS, vol. 6361, pp. 45–52. Springer, Heidelberg (2010)
8. Manniesing, R., Viergever, M.A., Niessen, W.J.: Vessel Enhancing Diffusion: A Scale Space Representation of Vessel Structures. Med. Image Anal. 10, 815–825 (2006)
9. Weickert, J.A.: Coherence-Enhancing Diffusion Filtering. Int. J. Comput. Vis. 31, 111–127 (1999)
10. Mendrik, A.M., Vonken, E.J., Rutten, A., Viergever, M.A., van Ginneken, B.: Noise Reduction in Computed Tomography Scans Using 3-D Anisotropic Hybrid Diffusion with Continuous Switch. IEEE Trans. Med. Imaging 28, 1585–1594 (2009)

Appendix A

Parameters design:

Table 2. The parameters in optimization stage: σ (Gaussian scale); C (contrast constant); λ, λ_c, λ_e (contrast parameters to RPM, CED and EED); τ (time step); η: (number of iteration).

Filter	Abbr	Parameter optimization values
Regular Perona- Malik	RPM	τ: 0.0625; σ: 0.5, 1; τ: 0.0625 η: 4, 8, 12, 16, 18, 20, 22, 24, 30 40, 50 ; λ: 5, 10, 12, 14, 16, 18, 20, 25, 30, 80, 150;
Edge-Enhancing Diffusion	EED	σ: 0.5, 1; C: 3.31488; τ: 0.0625 λ_e: 5, 10, 30, 80, 120, 160 η : 4, 8, 12, 16, 20, 24, 30, 35 ,40 45, 50
Coherence-Enhancing Diffusion	CED	σ: 0.5, 1; ρ: 0.5, 1; τ: 0.0625; α: 0.001 λ_c: 5,10, 30, 80, 120, 160 η: 4, 8, 12, 16, 22, 26, 30, 35, 40, 45, 50
Hybrid Diffusion filter with Continuous Switch	HDCS	σ: 0.5, 1; ρ: 0.5, 1; α: 0.001 λ_h: 5, 10, 15, 20, 30 λ_c: 5; λ_e: 10 η: 4, 8, 12, 16, 20, 25, 30, 40, 50
Vessel Enhancing Diffusion	VED	σ: 1 – 3 (5 scales); τ: 0.0625 α: 0.5; β: 0.5; γ: 10, 40, 80, 120, 160, 280 η: 4, 8, 12, 16, 20, 25, 32, 40, 50 ω: 8, 25, 32 s : 0.5, 1, 2, 5 ε: 0.01; c: 10^{-6}

*Contrast parameters in HDCS can be used form EED and CED.